Dual-Tone Radio Interferometric Ranging Using PXI

Jie Huang, Yiyin Wang, Li'an Li, Xinping Guan
Department of Automation
Shanghai Jiao Tong University
Shanghai, China
E-mails: jhuang19921020@gmail.com
{yiyinwang, li_li_an, xpguan}@sjtu.edu.cn

Marie Shinotsuka
School of Electrical & Computer Engineering
Georgia Institute of Technology
Atlanta, USA
E-mails: gtg594x@mail.gatech.edu

***Abstract*—Accurate location information is crucial for wireless sensor networks (WSNs). It is quite challenging to achieve a balance between localization accuracy and cost. Recently, a dual-tone radio interferometric positioning system (DRIPS) and a DRIPS with undersampling techniques (uDRIPS) are proposed, respectively. Thanks to the special design of the dual-tone signal, both DRIPS and uDRIPS are robust to flat-fading channels. They provide promising options to achieve high accuracy with low cost. In this paper, we evaluate the performance of the ranging algorithms of DRIPS and uDRIPS using National Instruments' PCI eXtensions for Instrumentation (NI PXI). Although both DRIPS and uDRIPS employ the same dual-tone signal, their ranging methods are different. DRIPS extracts the range-related phase information of a low-frequency signal created by squaring the received dual-tone signal, while uDRIPS directly samples the received dual-tone signal to estimate the phase information. The experimental results show that the average errors of the ranging algorithms of uDRIPS and DRIPS can be as small as 11 cm at a range of 5 m. Moreover, the ranging performance of uDRIPS outperforms that of DRIPS, as the squaring operation in DRIPS amplifies the noise.**

***Keywords*—dual-tone signal; localization; PXI; range estimate**

I. INTRODUCTION

Location-aware services are quite important for most WSN applications. There are a lot of range-based localization systems that have been proposed. Global Positioning System (GPS) is well used in outdoor environments, and it can achieve a positioning accuracy of 5 m [1]. However, its performance for indoor environments is inferior because it is difficult for satellite radio signals to penetrate buildings. Moreover, the ultra-wideband (UWB) localization systems [2] have high accuracy, but the high cost discourages their popularity.

The radio interferometric positioning system (RIPS) proposed in [3] utilizes two transmitters to create the interferometric signal directly. The frequencies of the two transmitters are close. Thus, the interferometric signal has a low-frequency envelope, which can be measured by cheap hardware readily available on a WSN node. The phase of the signal is used to obtain the Q-range, which is determined by the relative positions of transmitters and receivers. However, the RIPS only accommodates additive white Gaussian noise (AWGN) channels, and it faces the integer ambiguity issue. Furthermore, the amplified noise due to the squaring operation degrades the ranging performance. RIPS is used for tracking mobile nodes in [4], [5]. In these tracking systems, Doppler shifts are exploited in velocity estimates and positioning. Radio interferometric angle of arrival (AOA) estimation is proposed in [6]. It groups three nodes together to form an antenna array, and the measured phase differences are transformed into the AOAs to acquire the target position. In [7] an AOA-assisted relative interferometric localization method is proposed and implemented with software defined radios. An FPGA-based RIPS developed in [8] provides a more robust and flexible platform. The stochastic RIPS proposed in [9] makes use of radios at 2.4 GHz. An asynchronous RIPS (ARIPS) is designed in [10] to deal with random phase due to asynchronous oscillators. Nevertheless, the ARIPS can also only accommodate AWGN channels. Recently, a dual-tone radio interferometric positioning system (DRIPS) is proposed in [11] to combat the flat-fading channels. However, it employs the squaring operation to produce a low-frequency differential signal, which results in a high noise power. A DRIPS with undersampling techniques (uDRIPS) is further proposed in [12] to avoid noise amplification by directly sampling the received dual-tone signal. The uDRIPS is robust to flat-fading channels as well.

In this paper, we employ National Instruments' PCI eXtensions for Instrumentation (NI PXI) [13] to implement and evaluate the ranging methods proposed in DRIPS and uDRIPS, respectively. In the experiments, we use NI PXIe-5673e (NI 5673) as a transmitter, and NI PXIe-5663e (NI 5663) as a receiver. The transmitter emits a dual-tone signal, whose frequency difference is smaller than the channel coherence bandwidth. At the receiver, the ranging methods of DRIPS and uDRIPS are employed to extract the time-of-arrival (TOA) plus an unknown parameter from the received signal. The unknown parameter is composed of an unknown integer due to phase wrapping and an offset due to the unknown transmission time. This unknown parameter is calibrated at the beginning of each ranging session. The complementary cumulative distribution function (CCDF) curves of the absolute error demonstrate the ranging performance under different system parameter setups. The results show that the average errors of both algorithms can be as small as 11 cm at a range of 5 m. Furthermore, the ranging performance of uDRIPS outperforms that of DRIPS as the squaring operation in DRIPS amplifies the noise.

The rest of the paper is organized as follows. In Section II, the system model is introduced. The ranging algorithms of uDRIPS and DRIPS are reviewed in Section III, respectively. We briefly discuss the error sources in Section IV. In Section V, the implementation and evaluation of the ranging methods for DRIPS and uDRIPS using PXI are discussed. The conclu-

978-1-63190-077-8

sions are drawn at the end of this paper.

II. System Model

In the experiments, only a single transmitter-receiver pair is used in the ranging measurements. The transmitter emits a dual-tone signal as

$$s(t) = ae^{j\varphi}e^{j2\pi(f_c+f_b)t}(1+e^{j2\pi g_b t}), \tag{1}$$

where a is the amplitude of the signal, φ is the unknown initial phase offset, f_c is the carrier frequency, f_b is the frequency of the first tone and f_b+g_b is for the second one, where the frequency difference g_b is set to be small but greater than zero.

The frequency difference g_b is designed to be smaller than the channel coherence bandwidth. Therefore, the two tones of the dual-tone signal experience the same channel fading effect [14]. The channel fading effect can be canceled out in the ranging algorithms. Thus, uDRIPS and DRIPS are robust to flat-fading channels. The received signal is then down converted by f_c, which is modeled as

$$r(t) = \beta s(t-t_0-\tau)e^{-j2\pi f_c t+j\eta}+\omega(t), \tag{2}$$

where β is the complex channel coefficient attributing to the flat-fading channel effect, and it can be modeled as a zero-mean complex Gaussian random variable. The unknown t_0 represents the unknown transmission time as the transmitter and the receiver are not synchronized. Moreover, τ is the propagation delay, η is the unknown initial phase due to the randomness of the local oscillator, and $\omega(t)$ is a noise term that can be viewed as zero-mean complex Gaussian random process. By plugging (1) into (2), we arrive at

$$r(t) = \alpha\beta e^{j2\pi f_b t}e^{j\theta}(1+e^{j2\pi g_b t}e^{j\phi})+\omega(t), \tag{3}$$

where $\alpha = ae^{j(\varphi+\eta)}$, $\theta = -2\pi(t_0+\tau)(f_c+f_b)$, and $\phi = -2\pi g_b(t_0+\tau)$. The parameter τ in ϕ is of interest, because it is related to the distance between the transmitter and the receiver as $d = c\tau$, where c is the speed of light. Note that ϕ can be decomposed as an integer part and a fractional part as follows

$$\phi = \psi + 2\pi k, \tag{4}$$

where ψ is in the range of $[-\pi,\pi)$ $(-\pi \le \psi < \pi)$. and k is an integer. The estimated phase based on the received signal is $\hat{\psi}$ instead of $\hat{\phi}$.

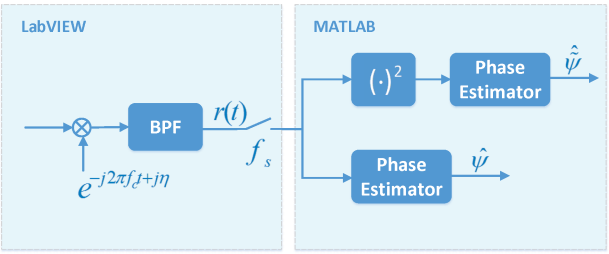

Fig. 1: The signal processing at the receiving end on PXI.

III. Ranging Methods

The received signal is first down converted and bandpass filtered. Then the signal is sampled and used to estimate the phase ψ by uDRIPS and DRIPS as shown in Fig. 1. In order to compare the performance of the ranging algorithms of uDRIPS and DRIPS, we set the sampling frequency in uDRIPS and DRIPS to be the same, and the sampling frequency $f_s > 2(f_b+g_b)$. The ranging algorithms of the uDRIPS and the DRIPS are introduced in the following subsections, respectively.

A. uDRIPS:Phase Estimation With Undersampling Techniques

At the receiver, $r(t)$ is sampled at the rate f_s. From now on, we ignore the noise term for simplicity. The N samples of the signal $r(t)$ are collected into a vector $\mathbf{r}$, which is modeled as

$$\mathbf{r} = \mathbf{A}\mathbf{x}, \tag{5}$$

where $\mathbf{A} = [\mathbf{\Phi}(f_b/f_s)\ \ \mathbf{\Phi}((f_b+g_b)/f_s)]$ with $\mathbf{\Phi}(f) = [1, e^{j2\pi f}, \ldots, e^{j2\pi(N-1)f}]^T$, and $\mathbf{x} = \alpha\beta[e^{j\theta}, e^{j(\theta+\phi)}]^T$. Applying the least-squares (LS) method, $\mathbf{x}$ can be given by

$$\hat{\mathbf{x}} = \mathbf{A}^{\dagger}\mathbf{r}, \tag{6}$$

where $(\cdot)^{\dagger}$ denotes the pseudo-inverse. Due to the phase wrapping, the phase ψ can be estimated as

$$\hat{\psi} = \arg\{[\hat{\mathbf{x}}]_1^*[\hat{\mathbf{x}}]_2\}, \tag{7}$$

where $(\cdot)^*$ denotes the complex conjugate, $\arg(\cdot)$ denotes the argument of a complex number, and $[\mathbf{a}]_n$ is the nth element of the vector $\mathbf{a}$.

B. DRIPS:Phase Estimation With Squaring Operation

In DRIPS, let the vector $\mathbf{r}$ make a element-wise multiplication (denoted by $\odot$) with its complex conjugate, and we obtain

$$\mathbf{q} = \mathbf{r}\odot\mathbf{r}^*. \tag{8}$$

Substituting the sampled $r(t)$ into (8), we arrive at

$$\mathbf{q} = 2a^2|\beta|^2\mathbf{1}_N + \mathbf{v}, \tag{9}$$

where $(2a^2|\beta|^2)\mathbf{1}_N$ is the DC component, and $\mathbf{1}_N$ is an all-one column vector of length N. The phase ϕ is included in $\mathbf{v}$, and $\mathbf{v} = 2a^2|\beta|^2[\cos(\phi), \cos(2\pi g_b/f_s+\phi), \ldots, \cos(2(N-1)\pi g_b/f_s+\phi)]^T$. After getting rid of the DC component, $\mathbf{v}$ can be obtained and characterized as

$$\mathbf{v} = \tilde{\mathbf{A}}\tilde{\mathbf{x}}, \tag{10}$$

where $\tilde{\mathbf{A}} = [\mathbf{\Phi}(-g_b/f_s)\ \ \mathbf{\Phi}(g_b/f_s)]$, and $\tilde{\mathbf{x}} = a^2|\beta|^2[e^{-j\phi}, e^{j\phi}]^T$. Similarly to the uDRIPS, the LS method is applied to estimate $\tilde{\mathbf{x}}$ that is given by

$$\hat{\tilde{\mathbf{x}}} = \tilde{\mathbf{A}}^{\dagger}\mathbf{v}, \tag{11}$$

due to the phase wrapping, the estimated phase ψ is

$$\hat{\tilde{\psi}} = \frac{1}{2}\arg\{[\hat{\tilde{\mathbf{x}}}]_1^*[\hat{\tilde{\mathbf{x}}}]_2\}. \tag{12}$$

where $\hat{\tilde{\psi}}$ denotes the phase estimate of ψ for DRIPS.

In order to acquire the range estimates, we need to estimate the parameter τ in ϕ. However, it is difficult for us to obtain phase ϕ by ψ directly due to the unknown k. Since t_0 and

$2\pi k$ are both unknown, we bundle them as $u = t_0 + k/g_b$ and arrive at

$$\hat{\psi} = -2\pi g_b(u + \tau), \tag{13}$$

where we connect phase ψ with propagation delay τ. Thus, the delay estimate is given by

$$\hat{\tau} = -\hat{\psi}/(2\pi g_b) - u. \tag{14}$$

IV. Source Of Error

There are various error sources that degrades the ranging performance of the two systems. This section is to briefly discuss these sources of errors, further research is necessary to properly deal with these errors. The sources of errors are as follows:

Frequency offset—the frequency difference between the transmitter and receiver. Although the transmitter-receiver pair shares the same frequency reference clock, there is still a tiny frequency offset between them. The frequency of the first tone f_b and the frequency difference g_b are involved in solving the TOA for range estimation in uDRIPS. The frequency difference g_b is also involved in solving TOA in DRIPS. The offsets of f_b and g_b result in an error in estimating τ.

Frequency drift and phase noise—the phase noise and drift of the actual frequency of the signal. The frequencies f_b and g_b are assumed to be stable as we use the specified frequencies in calculation. However, phase noise and frequency drift are inevitable. In the experiments, 100 phase estimates takes 5 s, thus the frequency drift is negligible. Nevertheless, the phase noise may have a significant effect on the range estimates.

Transmission time t_0 inaccuracy—the difference between the estimated and actual t_0 of the transmitted signal. The unknown transmission time t_0 is estimated by the first 20 range estimates with true distance, and the difference between the estimated and actual t_0 will result in an error in range estimates.

Signal-to-Noise Ratio—the signal strength relative to noise of the $r(t)$ signal. As SNR mainly depends on the physical distance between the transmitter and the receiver, the error increases with the increase of the distance.

V. Implementations And Evaluation

As shown in Fig. 2, the transmitter NI 5673 and the receiver NI 5663 are the RF vector signal generator and analyzer, respectively. The controller is a NI PXIe-8133 (NI 8133) with 1.73 GHz Quad-Core embedded. It can modify the transmitting signal and analyze the received signal. These components of PXI are all inserted into the chassis PXIe-1075 (NI 1075), where a frequency reference clock is provided.

The frequency ranges of NI 5673 and NI 5663 are 50 MHz $\sim$ 6.6 GHz and 10 MHz $\sim$ 6.6 GHz, respectively. Since they use the same clock source, we can assume the frequency drift between NI 5673 and NI 5663 is negligible. NI LabVIEW is employed to program NI 5663 and NI 5673. After receiving and sampling signals, the PXI handle the data with the ranging algorithms of uDRIPS and DRIPS to estimate the phase ψ. Since LabVIEW can call the MATLAB software to execute

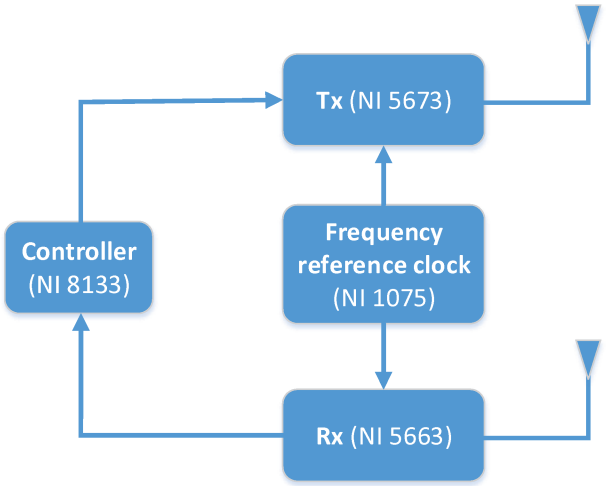

Fig. 2: PXI components for the ranging system.

scripts, MATLAB script is used in LabVIEW to perform the range estimations.

The experiments are conducted in a lab. The frequency of the first component of the dual-tone signal is that $f_b = 200$ kHz, and the sampling frequency $f_s = 2$ MHz$> 2(f_b+g_b)$. we set the number of samples $N = 100000$ and $(Ng_b)/f_s = 2500$ is an integer, which makes sure that the samples we collected are integer multiple of the period. As a result, the DC component can be obtained by an average operation of these samples, and then be eliminated in DRIPS. As the transmitter-receiver pair shares the same frequency reference clock, we use the specified value of f_b and g_b in ranging estimation at the receiver. The ranging experiments are conducted 500 times and we fetch N samples to estimate the phase ψ every time, as a result, 500 range estimates are obtained. The first 20 range estimates are used to acquire the unknown value u. After the calibration with u, we can estimate τ to obtain the distance d. In the experiments, we mainly focus on three parameters, namely, the frequency difference g_b, the distance to be measured d, and the carrier frequency f_c. Therefore, comparison experiments are carried out when one of them varies and the other two are fixed, and the results show how they affect the ranging performance.

A. Ranging At Different Frequency Differences

The frequency difference g_b is an important parameter as it is involved in (14). There is a tradeoff in choosing a proper g_b. A small g_b results in a small phase ψ, however, it is difficult for PXI to acquire a high precision phase. On the other hand, a large g_b may exceed the channel coherence bandwidth, which violates the flat-fading channel model. To intuitively display the performance, the complementary cumulative distribution function (CCDF) curves of the absolute distance errors are employed. As shown in Fig. 3, the performance of $g_b = 50$ kHz (the magenta line) is obviously better than that of $g_b = 10$ kHz (the blue line). Therefore, we set $g_b = 50$ kHz in the following two comparison experiments.

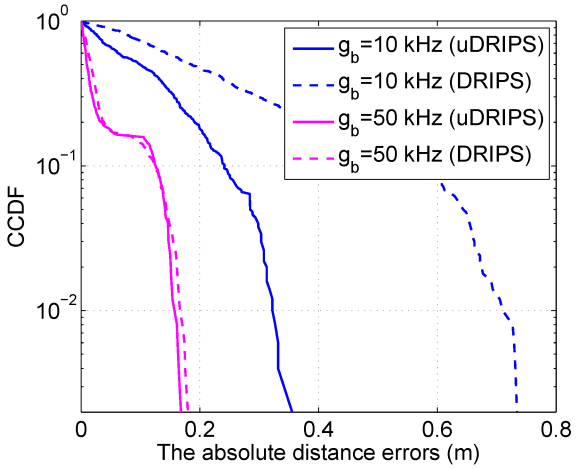

Fig. 3: The CCDF curves of the absolute distance errors at different frequency differences with $d = 1$ m, $f_c = 446$ MHz.

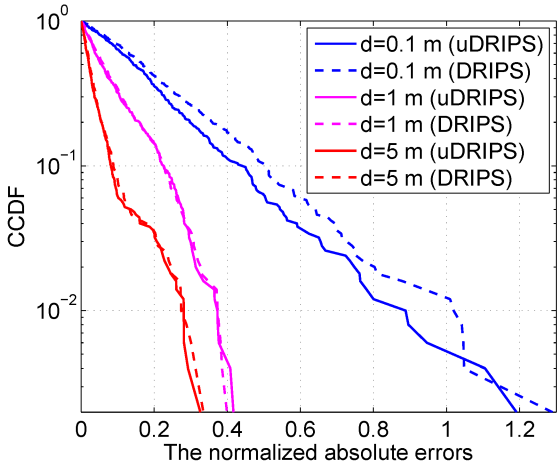

Fig. 4: The CCDF curves of the normalized absolute distance errors at different distances with $f_c = 446$ MHz, $g_b = 50$ kHz.

B. Ranging At Different Distances

We choose 446 MHz as the carrier frequency when the distance changes. Table I shows the mean error (ME), the median absolute error (MAE) and the root mean square error (RMSE) of the estimated distances under different true distances. Although the ME of the DRIPS at the distances of 1 m and 5 m are better than that of uDRIPS, the RMSE and the MAE of the DRIPS are worse. The error increases with the distance, because farther distance results in low signal-to-noise ratio (SNR). On the other hand, the CCDF curves of the normalized absolute errors ($|\hat{d}-d|/d$) of different distances are shown in Fig. 4. The estimation using the uDRIPS (the solid lines) achieves slightly better performance than the one using the DRIPS (the dashed lines). Moreover, the farther distance has a lower normalized error as shown in Fig. 4, as the similar error for different distances due to the frequency offset and phase noise indicate a larger normalized error with a decreased distance.

TABLE I: The ME, MAE and RMSE of uDRIPS and DRIPS at different distances.

Distance (cm)	**Method**	**ME (cm)**	**MAE (cm)**	**RMSE (cm)**
10	uDRIPS	0.37	1.42	2.60
	DRIPS	0.41	1.69	3.00
100	uDRIPS	1.02	5.56	12.39
	DRIPS	0.68	6.14	12.55
500	uDRIPS	-10.62	10.74	29.61
	DRIPS	-10.24	11.45	31.11

C. Ranging At Different Carrier Frequencies

We also evaluate the ranging performance of the DRIPS and the uDRIPS with different carrier frequencies at the distance 1 m. Table II shows the ME, MAE and RMSE of the estimated distances at different carrier frequencies. We can see that all performance indicators of the uDRIPS are better than the DRIPS. It is also clear from Table II that the estimation errors increase with the carrier frequency. We also employ the CCDF curves of the absolute distance errors to show the performance of DRIPS and uDRIPS directly. As displayed in Fig. 5, the performance of the $f_c = 500$ MHz (the blue line) is much better than the other two carrier frequencies, and the performance of $f_c = 1$ GHz (the magenta line) is slightly better than $f_c = 2.4$ GHz (the red line). Furthermore, it is clear that uDRIPS outperforms DRIPS at all tested carrier frequencies.

TABLE II: The ME, MAE and RMSE of uDRIPS and DRIPS at different carrier frequencies with $d = 1$ m, $g_b = 50$ kHz.

Carrier Frequency (Hz)	**Method**	**ME (cm)**	**MAE (cm)**	**RMSE (cm)**
500M	uDRIPS	0.64	1.37	2.32
	DRIPS	-0.88	1.97	3.00
1G	uDRIPS	-1.53	4.00	10.07
	DRIPS	-1.68	4.51	10.19
2.4G	uDRIPS	-5.80	7.11	9.92
	DRIPS	-6.48	8.03	10.27

VI. Conclusions

In this paper, we implement and evaluate the ranging algorithms of uDRIPS and DRIPS by PXI. The special design of the dual-tone signal allows the systems to accommodate flat-fading channels. We use specified frequencies f_b and g_b to do the range estimates in later experiments for their performance. The experiments are carried out at different frequency differences, distances and carrier frequencies. The results show that the average error of both ranging algorithms can achieve about 11 cm at a range of 5 m. When the distance is 1 m, the average error of both ranging algorithms can achieve less than

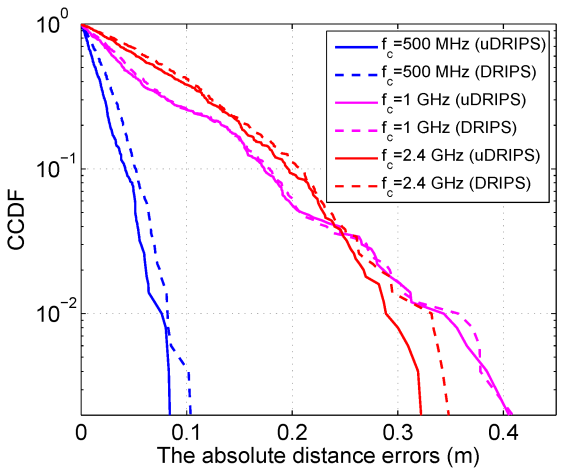

Fig. 5: The CCDF curves of the absolute distance errors at different carrier frequencies with $d = 1$ m, $g_b = 50$ kHz.

1 cm at the carrier frequency of 500 MHz. As the squaring operation of DRIPS amplifies the noise power, uDRIPS has a better performance than DRIPS.

REFERENCES

[1] E. D. Kaplan and C. J. Hegarty, *Understanding GPS: principles and applications*. Artech house, 2005.

[2] S. Gezici, Z. Tian, G. B. Giannakis, H. Kobayashi, A. F. Molisch, H. V. Poor, and Z. Sahinoglu, "Localization via ultra-wideband radios: a look at positioning aspects for future sensor networks," *IEEE Signal Processing Magazine*, vol. 22, no. 4, pp. 70–84, 2005.

[3] M. Maróti, P. Völgyesi, S. Dóra, B. Kusỳ, A. Nádas, Á. Lédeczi, G. Balogh, and K. Molnár, "Radio interferometric geolocation," in *Proc. ACM SenSys*, San Diego, CA, USA, Nov. 2005, pp. 1–12.

[4] B. Kusy, J. Sallai, G. Balogh, A. Ledeczi, V. Protopopescu, J. Tolliver, F. DeNap, and M. Parang, "Radio interferometric tracking of mobile wireless nodes," in *Proc. ACM MobiSys*, San Juan, Puerto Rico, Jun. 2007, pp. 139–151.

[5] B. Kusy, A. Ledeczi, and X. Koutsoukos, "Tracking mobile nodes using rf doppler shifts," in *Proc. ACM SenSys*, Sydney, Australia, Nov. 2007, pp. 29–42.

[6] I. Amundson, J. Sallai, X. Koutsoukos, and A. Ledeczi, "Radio interferometric angle of arrival estimation," in *Wireless Sensor Networks*. Springer, 2010, pp. 1–16.

[7] J. Friedman, A. Davitian, D. Torres, D. Cabric, and M. Srivastava, "Angle-of-arrival-assisted relative interferometric localization using software defined radios," in *Proc. IEEE MILCOM*, Boston, MA, USA, Oct. 2009, pp. 1–8.

[8] S. Szilvási, J. Sallai, I. Amundson, P. Volgyesi, and A. Lédeczi, "Configurable hardware-based radio interferometric node localization," in *Proc. IEEE Aerospace Conf.*, Big Sky, USA, Mar. 2010, pp. 1–10.

[9] B. Dil and P. J. Havinga, "Stochastic radio interferometric positioning in the 2.4 ghz range." in *Proc. ACM SenSys*, Seattle, WA, USA, Nov. 2011, pp. 108–120.

[10] Y. Wang, M. Shinotsuka, X. Ma, and M. Tao, "Design an asynchronous radio interferometric positioning system using dual-tone signaling," in *Proc. IEEE WCNC*, Shanghai, China, Apr. 2013, pp. 2294–2298.

[11] Y. Wang and X. Ma, "Designing dual-tone radio interferometric positioning systems," Georgia Inst. Technol., Atlanta, GA, USA, Tech. Rep., May 2013.

[12] Y. Wang, L. Li, X. Ma, M. Shinotsuka, C. Chen, and X. Guan, "Dual-tone radio interferometric positioning systems using undersampling techniques," *IEEE Signal Processing Letters*, Jun. 2014, accepted.

[13] National Instruments' PCI eXtensions for Instrumentation (NI PXI). National Instruments. [Online]. Available: http://www.ni.com/pxi/

[14] J. Proakis and M. Salehi, *Digital Communications*, 5th ed. New York, NY, USA: McGraw-Hill, 2007, vol. 3.